

Short communication

Vibrational analysis of lithium nickel vanadate

M.S. Bhuvaneshwari^a, S. Selvasekarapandian^{a,*}, O. Kamishima^b,
J. Kawamura^b, T. Hattori^b

^a *Solid State and Radiation Physics Laboratory, Department of Physics, Bharathiar University, Coimbatore 641046, India*

^b *Institute of Multidisciplinary Research for Advanced Materials, Tohoku University, Sendai, Japan*

Received 12 May 2004; accepted 13 July 2004

Available online 16 September 2004

Abstract

The compound Li_XNiVO_4 ($X = 0.8, 1.0, 1.2$) is prepared by a solid-state reaction method. The vibrational analysis of the compound is studied using Fourier transform infra red (FTIR) and Raman spectroscopic techniques. A new peak at 1039 cm^{-1} is observed for $\text{Li}_{1.2}\text{NiVO}_4$ in the FTIR analysis and indicates the presence of $\text{Li}^+-\text{O}-\text{V}$ bond interactions. The FTIR and Raman characteristic bands for cubic inverse spinel structure are observed for all samples. Using the diatomic approximation method, the bond length and the bond order of the compound with various Li compositions are calculated. The valence state of the compounds is calculated using the Pauling valence sum rule and is found to be nearly 5.2 for all compositions of Li_XNiVO_4 ($X = 0.8, 1.0, 1.2$).

© 2004 Elsevier B.V. All rights reserved.

Keywords: Lithium nickel vanadate; Raman spectroscopy; FTIR analysis; Diatomic approach; Pauling valence sum rule; Rechargeable lithium batteries

1. Introduction

The development of new electrode materials for rechargeable lithium cells has received a considerable attention because of the demand for portable power sources with high specific energy [1,2]. Among them, lithium nickel vanadate has attracted particular attention because of its high specific energy and its ability to be used both as a cathode and as an anode material [3,4]. This latter attribute is due to the unusual inverse spinel structure, which is different from the crystal structures of other lithium incorporated materials [5,6]. To date, numerous preparation methods have been reported but they offer no great improvements in the cell performance of LiNiVO_4 or related materials such as LiCoVO_4 [7]. It has also been suggested [7,8] that further research on the structure and valence of these materials would be promising due to their potential cathode

and anode applications. In the present study, therefore, the structure and valence state of Li_XNiVO_4 ($X = 0.8, 1.0, 1.2$) have been studied by means of Fourier transform infra red (FTIR) and Raman spectroscopy vibrational techniques. The investigation uses Raman spectroscopy to analyze the bond strength, bond order and valence state of Li_XNiVO_4 ($X = 0.8, 1.0, 1.2$). The Raman vibration spectrum directly probes the structure and bonding of a transition–metal oxide complex, and consequently can be used to discriminate between alternate molecular structures proposed for a given chemical species [9]. Hardcastle and Wachs [10] demonstrated that the diatomic approach is a versatile tool for interpreting Raman spectra because it assumes that vibrational interactions between neighboring chemical bonds in complex transition oxides may be neglected. This assumption suggests that a direct relation exists between a metal–oxygen bond length and its Raman stretching frequency and, therefore, metal oxygen bond lengths may be directly determined from the measurement of Raman stretching frequencies. Hence, in the present study, this diatomic approach has been used to calculate the bond order, bond length and valence

* Corresponding author. Tel.: +91 422 242222x422;
fax: +91 422 2422387.

E-mail address: sekarapandian@yahoo.com (S. Selvasekarapandian).

state of lithium nickel vanadate compounds with various Li compositions.

2. Experimental

Lithium nickel vanadate, Li_XNiVO_4 ($X = 0.8, 1.0, 1.2$) was prepared by a solid-state reaction method. The stoichiometric amounts of the raw materials Li_2CO_3 , NiO and V_2O_5 according to the compositions of Li_XNiVO_4 ($X = 0.8, 1.0, 1.2$) were ground into fine powder using a mortar and pestle. The resultant powder was heated at a temperature of 1073 K in a porcelain crucible. Fourier transform (FTIR) measurements were performed with a Bruker IFS – 66 V instrument. Raman spectra of the samples were obtained with a microscopic Raman spectrometer using the Ar ion laser line of 4880 Å. Lorentzian line shapes were fitted to the Raman spectra, both for the samples and for all compositions for which the peak position of the Raman peak were obtained.

3. Diatomic approximation theory

Hardcastle and Wachs [11] reported that the diatomic approach could be used to interpret Raman spectra of a vanadium oxide compound in terms of V–O bond lengths [11]. This approach differs from other models. In the site symmetry approach, for example, each metal polyhedron is separated from the crystalline lattice and therefore does not directly yield structural details. According to the diatomic approach, as a first approximation, the Raman spectrum of crystalline

metal oxide is a superposition of the stretching frequencies from an assembly of metal–oxygen diatomic oscillators [11]. Each oscillator has a unique inter-atomic distance and a unique stretching force constant, and also exhibits a unique vibrational band. If the metal–oxygen bond is assumed to act like harmonic oscillator, then the stretching force constant may be found from its square-root dependence on vibrational frequency [11]. Hence, according to the diatomic approach, as given by Hardcastle et al., the correlation between bond length (R) and stretching frequency (ν) is:

$$\nu = 21349 \exp(-1.9176 R) \quad (1)$$

where ν is in cm^{-1} and R is in Å. The bond length or inter-atomic distance and the bond order or bond valence (s) are calculated using the relationship developed by Brown and Wu [12]. This equation relates the cation–oxygen bond order to the bond length. The empirical expression relating a V–O bond length to its bond valence for pentavalent V is given by:

$$s(\text{V–O}) \approx \left(\frac{R}{1.791} \right)^{-5.1} \quad (2)$$

where 1.791 Å is the estimated bond length for a V–O bond of unit valency for V^{5+} cations. The empirical parameters 1.791 and 5.1 are determined based on data from a larger number of V^{5+} environments [12].

The valance state of vanadium is calculated from the Pauling valence sum rule. The Pauling bond strength, also referred to as bond order or bond valence, reflects the relative strength of a chemical bond and shows the distribution of available valence electrons in the chemical bonding of molecular species

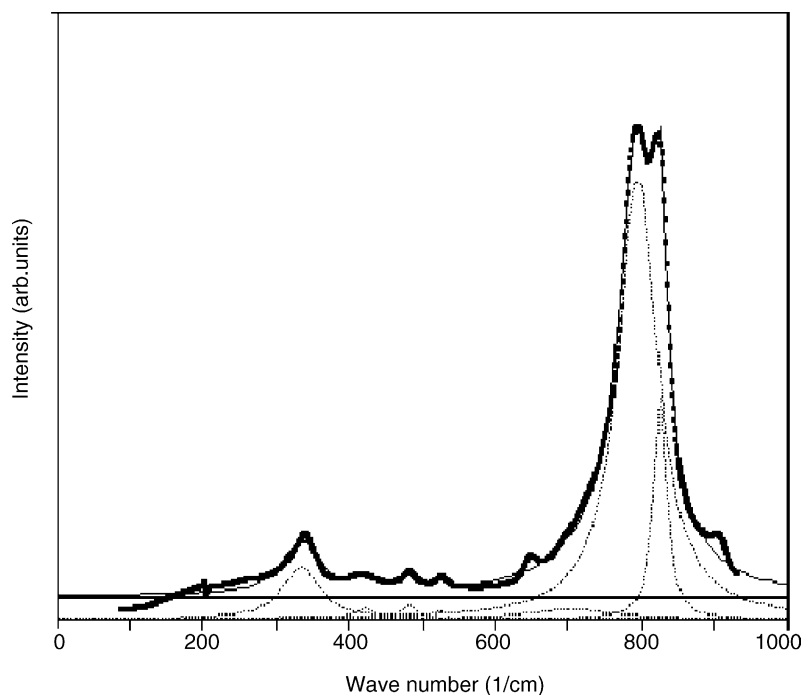


Fig. 1. Raman spectrum for $\text{Li}_{0.8}\text{Ni}_4\text{VO}_4$.

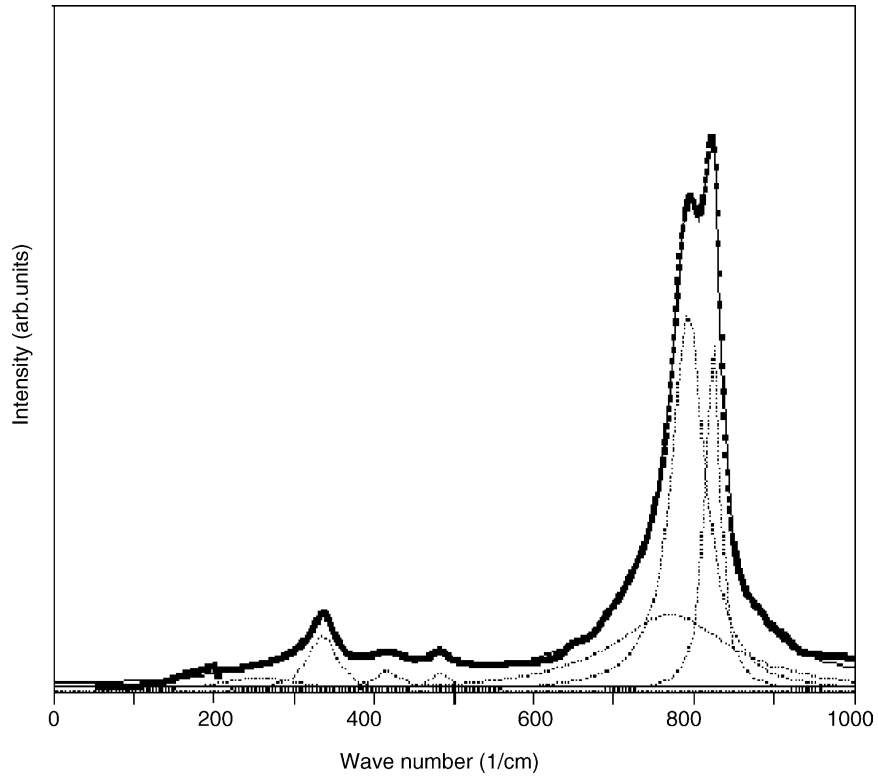


Fig. 2. Raman spectrum for $\text{Li}_{1.0}\text{NiVO}_4$.

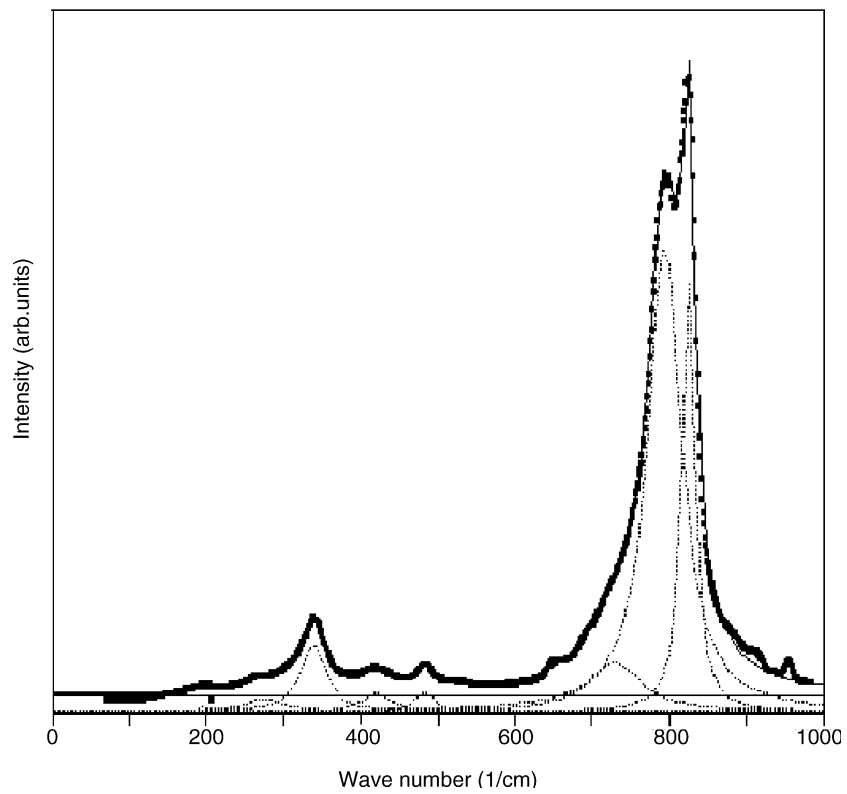


Fig. 3. Raman spectrum for $\text{Li}_{1.2}\text{NiVO}_4$.

[13]. Furthermore, it has been reported that according to the Pauling rule there is a conservation of valency associated with the metal cation. The valence sum rule is extremely useful in estimating the valence states of vanadium cations in vanadate structures. Hence, the calculated valence state has been compared with the formal oxidation state of vanadium cation [14]. The valence state of vanadium is calculated by adding the contributions from each V–O bond order as determined by Eq. (2).

4. Results and discussion

4.1. FTIR analysis

The FTIR spectra for all the three samples in the wave number range of 400–1200 cm^{-1} are presented in Fig. 4. The complex patterns of the bands observed at 630, 700 and at 810 cm^{-1} have been assigned to stretching vibrations of VO_4 tetrahedrons, and are found to be the characteristic vibrational bands of an inverse spinel structure [6]. Normally, the FTIR pattern observed in the 400–750 cm^{-1} region has been largely associated with the vibrations of NiO_6 and LiO_6 octahedral units or the bending vibrations of VO_4 tetrahedron. The bonding of Li and Ni with each oxygen atom in VO_4 tetrahedra introduces some asymmetry without disturbing the overall cubic symmetry of the elementary unit cell. Hence, the band at 810 cm^{-1} has also been assigned to the asymmetrical stretching modes in distorted VO_4 units. Two weak bands around 430 and at 420 cm^{-1} have been assigned to asymmetric stretching of Li–O in LiO_6 environments. These two peaks are more prominent for $\text{Li}_{1,0}\text{NiVO}_4$, compared with those for the other two samples. In addition, there are two small absorption peaks sited at around 1120 and at 1180 cm^{-1} ; these peaks tentatively belong to an asymmetry stretching vibrational mode of NiO_6 octahedra [8] and are similar for all three samples. For $\text{Li}_{1,2}\text{NiVO}_4$, a new small peak at about 1039 cm^{-1} is observed. This peak is absent for $\text{Li}_{0,8}\text{NiVO}_4$ and for $\text{Li}_{1,0}\text{NiVO}_4$. This is due to the concurrent existence of $\text{Li}^+\text{–O–V}$ bond interactions [15] since for $\text{Li}_{1,2}\text{NiVO}_4$ the Li composition is found to be very high compared with other samples. Hence, the FTIR spectrum for all samples indicates the presence of characteristic vibrational bands for the inverse spinel structure. Even though a new peak arises for $\text{Li}_{1,2}\text{NiVO}_4$, due to $\text{Li}^+\text{–O–V}$ interactions this will not produce a dramatic change in the structure of the compound, which has been inferred from the presence of characteristic vibrations for the inverse spinel structure.

4.2. Inverse spinel structure

The Raman spectra for lithium nickel vanadate with three different Li compositions are shown in Figs. 1–3. For compounds of the cubic spinel type, structure possesses prototype $\text{Fd}3\text{m}$ (O_h^7) symmetry and yields five Raman active modes symmetrical with the inversion centre ($\text{A}_{1\text{g}} + \text{E}_\text{g} +$

$3\text{F}_{2\text{g}}$) [16]. For lithium nickel vanadate, a strong broad band in the 700–850 cm^{-1} region is observed and is ascribed to the stretching frequencies of the VO_4 tetrahedron [7]. This may be due to the vibration between the oxygen and the highest valency cation (V^{5+}). This high-frequency peak has been observed at 823 cm^{-1} and is attributed to the stretching mode of the VO_4 tetrahedron with $\text{A}_{1\text{g}}$ symmetry, while the band located at 332 cm^{-1} is attributed to the bending mode of the VO_4 tetrahedron with E symmetry [9]. The broadness of the high frequency band may be associated with asymmetric bonding of the VO_4 tetrahedron. It has been reported that the Raman spectra for an ideal VO_4 tetrahedron should have a stretching frequency at around 796 cm^{-1} [17]. For lithium nickel vanadate, this band has been observed at 795 cm^{-1} for all Li compositions, which suggests an ideal VO_4 tetrahedron. The broadness of the high-frequency peak observed at 823 cm^{-1} for Li_xNiVO_4 increases with increase in Li composition. This may be due to the fact that two types of cations, Li and Ni, may be bonded to each oxygen atom of a VO_4 tetrahedron, as indicated by the FTIR analysis [7]. This asymmetry increases with increase in Li composition.

4.3. Diatomic approximation of calculating the valence state of vanadium

The procedure for making assignments of the Raman stretching frequencies as suggested by Hardcastle and Wachs [11] using diatomic approximation has been found to be very

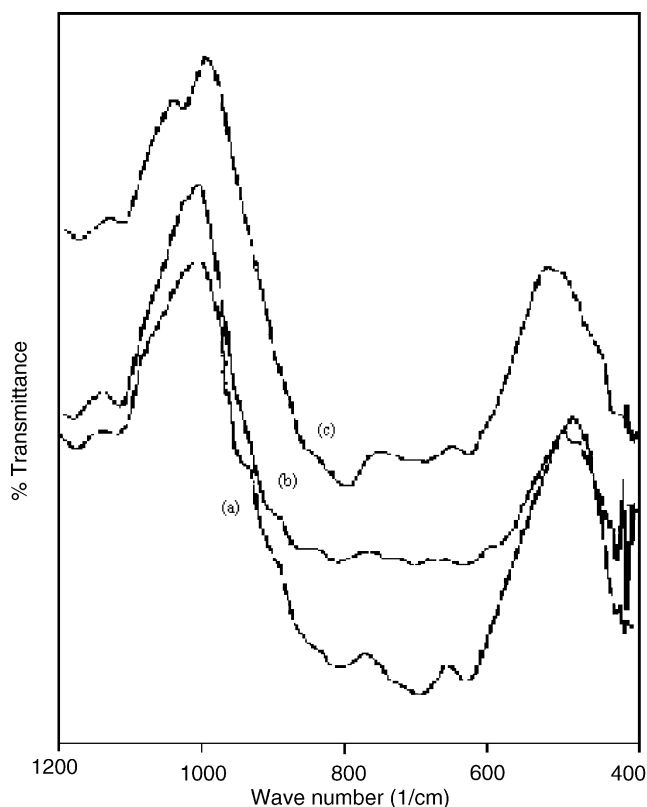


Fig. 4. FTIR spectrum for (a) $\text{Li}_{0,8}\text{NiVO}_4$, (b) $\text{Li}_{1,0}\text{NiVO}_4$, (c) $\text{Li}_{1,2}\text{NiVO}_4$.

Table 1
Vibrational modes observed in Raman spectrum for Li_XNiVO_4 ($X = 0.8, 1.0, 1.2$)

Samples	Raman (cm^{-1})	Bond length, R (Å)	Bond order, s (vu)	Assignment
$\text{Li}_{0.8}\text{NiVO}_4$	332 m	2.17	0.37	$\nu(\text{VO}_4)$
	420 w	2.04	0.51	$\nu(\text{Li}-\text{O})$
	648 w	1.82	0.91	$\nu(\text{Li}-\text{O}-\text{Ni})$
	795 vs	1.71	1.24	$\nu_{\text{ass}}(\text{VO}_4)$
	825 vs	1.69	1.31	$\nu_s(\text{VO}_4)$
$\text{Li}_{1.0}\text{NiVO}_4$	334 m	2.16	0.37	$\nu(\text{VO}_4)$
	420 w	2.04	0.51	$\nu(\text{Li}-\text{O})$
	655 sh	1.81	0.92	$\nu(\text{Li}-\text{O}-\text{Ni})$
	795 vs	1.71	1.24	$\nu_{\text{ass}}(\text{VO}_4)$
	825 vs	1.69	1.31	$\nu_s(\text{VO}_4)$
$\text{Li}_{1.2}\text{NiVO}_4$	337 m	2.16	0.38	$\nu(\text{VO}_4)$
	420 w	2.04	0.51	$\nu(\text{Li}-\text{O})$
	657 sh	1.81	1.08	$\nu(\text{Li}-\text{O}-\text{Ni})$
	795 vs	1.71	1.24	$\nu_{\text{ass}}(\text{VO}_4)$
	826 vs	1.69	1.32	$\nu_s(\text{VO}_4)$

w: – Weak; m – medium; sh – shoulder; vs – very strong; s – symmetric stretching; ass – asymmetric stretching.

simple. The short V–O bonds are assigned with terminal V=O bonds and vibrate at higher frequencies $>800\text{ cm}^{-1}$. Next, the V–O bonds of intermediate length, typical of bridging V–O bonds and having about unit valency, are assigned to Raman stretching frequencies in the $600\text{--}800\text{ cm}^{-1}$ region. In the present study, the stretching frequencies of the Li_XNiVO_4 ($X = 0.8, 1.0, 1.2$) samples are absorbed at around 790 and 823 cm^{-1} ; this feature is similar for all compositions of lithium nickel vanadate.

Using Eqs. (1) and (2), the bond length (R) and the bond valence has been calculated for both the samples and for different Li compositions. Using the Pauling valence sum rule, the valence state of vanadium in lithium nickel vanadate for three different Li compositions has been calculated using Eq. (2) and has been found to be nearly 5.2. The calculated bond valence and bond length for Li_XNiVO_4 ($X = 0.8, 1.0, 1.2$) are listed in Table 1. The same valence state for all compositions of Li suggests that there is no appreciable change in the structure with respect to Li composition within the composition range 0.8–1.0.

5. Conclusions

The compounds Li_XNiVO_4 ($X = 0.8, 1.0, 1.2$) have been prepared by a solid-state reaction method. FTIR and Raman structural analyses indicate the presence of characteristic vibrational bands for the inverse spinel structure for all the three samples. The bond order and bond valence have been calculated from the Raman stretching frequencies. The valence state of the samples calculated from the Pauling valence sum rule suggests that the oxidation state of vanadium in lithium nickel vanadate samples is nearly 5.2.

References

- [1] W. Chen, Q. Xu, Y.S. Hu, L.Q. Mai, Q.Y. Zhu, J. Mater. Chem. 12 (2002) 1926.
- [2] R.S. Liu, Y.C. Cheng, R. Gundakaram, L.Y. Jang, Mater. Res. Bull. 36 (2001) 1479–1486.
- [3] G.T.-K. Fey, W. Li, J.R. Dahn, J. Electrochem. Soc. 141 (1994) 2279.
- [4] S. Dennis, E. Baudrin, F. Orsini, G. Ourvard, M. Touboul, J.M. Tarascon, J. Power Sources 81–82 (1999) 79.
- [5] C.H. Lu, S.J. Liou, Ceram. Int. 25 (1999) 431–436.
- [6] P. Kalyani, N. Kalaiselvi, N. Muniyandi, Mater. Chem. Phys. 77 (2002) 662–668.
- [7] G.T.K. Fey, D.L. Huang, Electrochim. Acta 45 (1999) 295–341.
- [8] Q.Y. Lai, J.Z. Lu, X.L. Liang, F.Y. Yan, X.Y. Ji, Int. J. Inorg. Mater. 3 (2001) 381–385.
- [9] C. Julien, M. Massot, C.P. Vicente, Mater. Sci. Eng. B75 (2000) 6–12.
- [10] F.D. Hardcastle, I.E. Wachs, J. Raman Spectrosc. 21 (1990) 683.
- [11] F.D. Hardcastle, I.E. Wachs, J. Phys. Chem. 95 (1991) 5031–5041.
- [12] I.D. Brown, K.K. Wu, Acta Crystallogr. B32 (1976) 1957.
- [13] I.D. Brown, Chem. Soc. Rev. 7 (1978) 359.
- [14] R. Bacewicz, P. Kurek, Solid State Ionics 127 (2000) 151–156.
- [15] A. Surca, B. Orel, G. Drazic, B. Pihlar, J. Electrochem. Soc. 146 (1) (1999) 232–242.
- [16] S.R.S. Prabharan, M.S. Michael, S. Radhakrishnan, C. Julin, J. Mater. Chem. 7 (9) (1997) 1791–1796.
- [17] F.D. Hardcastle, I.E. Wachs, H. Eckert, D.A. Jefferson, J. Solid State Chem. 90 (1991) 194.